Cell. Mol. Life Sci. 66 (2009) 1434 – 1445
1420-682X/09/081434-12
DOI 10.1007/s00018-009-9038-1

Cellular and Molecular Life Sciences

Research Article

Basal autophagy is involved in the degradation of the ERAD component EDEM1

V. Le Fourn†, K. Gaplovska-Kysela†, B. Guhl, R. Santimaria, C. Zuber and J. Roth*

Division of Cell and Molecular Pathology, Department of Pathology, University of Zurich, Schmelzbergstr. 12, 8091 Zurich (Switzerland), Fax: +41-44-255-4407, e-mail: jurgen.roth@bluewin.ch

Received 15 January 2009; received after revision 16 February 2009; accepted 17 February 2009
Online First 7 March 2009

Abstract. Little is known about the fate of machinery proteins of the protein quality control and endoplasmic reticulum (ER)-associated degradation (ERAD). We investigated the degradation of the ERAD component EDEM1, which directs overexpressed misfolded glycoproteins to degradation. Endogenous EDEM1 was studied since EDEM1 overexpression not only resulted in inappropriate occurrence throughout the ER but also caused cytotoxic effects. Proteasome inhibitors had no effect on the clearance of endogenous EDEM1 in non-starved cells. However, EDEM1 could be detected by immunocytochemistry in autophagosomes and biochemically in LC3 immuno-purified autophagosomes. Furthermore, influencing the lysosome-autophagy pathway by vinblastine or pepstatin A/E64d and inhibiting autophagosome formation by 3-methyladenine or ATGs short interfering RNA knockdown stabilized EDEM1. Autophagic degradation involved removal of cytosolic Triton X-100-insoluble deglycosylated EDEM1, but not of EDEM1-containing ER cisternae. Our studies demonstrate that endogenous EDEM1 in cells not stressed by the expression of a transgenic misfolded protein reaches the cytosol and is degraded by basal autophagy.

Keywords. Autophagy, proteasome, protein quality control, protein, aggregates, EDEM1.

Introduction

The conformation of glycoproteins in the early secretory pathway is monitored by a quality control machinery [1, 2]. Non-native glycoprotein conformers are retained in the endoplasmic reticulum (ER) where they are exposed to the protein folding machinery. Terminally misfolded glycoproteins and excess subunits of heteromeric proteins are targeted for degradation by a process named ER-associated protein degradation (ERAD) [3, 4].

EDEM1 (ER degradation-enhancing α-mannosidase-like protein) and its yeast homologue Htmp1p are ERAD components that associate with ERAD substrates such as the Hong Kong variant of α1-antitrypsin [5–7]. It links the calnexin cycle to ERAD since EDEM1 overexpression caused accelerated release of mutant glycoproteins from calnexin and enhanced their clearance [6, 8, 9]. In addition, EDEM1 has been shown to interact with non-ERAD substrates such as endocytozed ricin and to be involved in its dislocation from the ER to the cytosol [10]. EDEM1 associates with Derlin-2 or -3 [11], two integral membrane proteins, which have been proposed to form part of the dislocation machinery for ERAD [12, 13]. These data indicate that EDEM1 is an ERAD component that is

† These authors equally contributed to this work.
* Corresponding author.

mainly involved in the transport of glycosylated ERAD substrates out of the ER [6, 8, 9, 14]. This is followed by their de-glycosylation by the cytosolic peptide:*N*-glycanase [15, 16] and degradation.

The degradation pathway of ERAD machinery proteins themselves, including that of EDEM1 [17], is poorly understood. However, EDEM1 has to be tightly regulated in the ER since otherwise all glycoproteins with mannose-trimmed *N*-glycans potentially would become EDEM1 substrates [5–7] in an indiscriminate manner and would be retained in the ER. This presumptive regulation is supported by our observation of the strikingly different subcellular distribution between endogenous and overexpressed EDEM1 [14]. Endogenous EDEM1, even in cells overexpressing the Hong Kong variant of α1-antitrypsin, is mostly present in ER-derived vesicles and the cytosol, whereas overexpressed EDEM1 is additionally detected throughout the entire ER.

Two main cellular degradative pathways are known to exist: the proteasomes and the lysosome-autophagy system. Proteasomes degrade polyubiquitin-tagged proteins after they have been unfolded by the proteasomal 19S cap [18]. Autophagy is the process that results in the lysosomal degradation of the cell's own constituents such as part of the cytoplasm (so-called macroautophagy) and organelles [19]. Basal autophagy is an important regulatory process through which the constitutive turnover of organelles and cytoplasmic proteins is accomplished. This was unequivocally shown in tissue-specific autophagy knockout mice [20–22]. Autophagy is not only an important cellular degradation mechanism [23], but also plays active roles in development, cancer and immune defense, and is a pre-condition for apoptosis [24–27]. Once autophagosomes are formed through the concerted action of different ATG gene products, they quickly fuse with lysosomes [28]. Autophagy can be induced or blocked by amino acid starvation or be triggered by ER stress enabling cells to return to regular metabolic states [29–31].

Using a combination of morphological and biochemical approaches, we show that endogenous EDEM1 in the cytosol, in the absence of induced cellular stress, is degraded by basal autophagy, and that overexpression of EDEM1 evokes cytotoxic effects. Thus, basal autophagy is involved in the degradation of EDEM1 by removing it from the cytosol.

Materials and methods

Cell culture and transient transfection. HepG2, HeLa and HEK293 cells (obtained from ATCC, Manassas, VA) were grown on glass coverslips to 25% confluency in MEM (Eagle, Gibco, Auckland, NZ) supplemented with 10% fetal bovine serum (FBS, Gibco) and 1.0 mM sodium pyruvate (Gibco) at 37°C in a humidified atmosphere of 5% CO_2. For transfection, cells were washed in Opti-MEM I (Invitrogen, Carlsbad, CA) and transfected for 5 h using FUGENE HD or FUGENE 6 (Roche Diagnostics, Mannheim, Germany; lipid/plasmid DNA ratio of 6:2). Each cell type was transfected with a mixture of CMV-EDEM1-p3xFLAG vector and pEGFP-C1-rat-endomannosidase-CMV vector [32] or with CMV-p3xFLAG control vector and pEGFP-C1-rat-endomannosidase-CMV vector at a ratio of 10:1. Cells were analyzed by immunofluorescence immediately following transfection or 1, 3 or 7 days after transfection to assess gene expression and cell morphology. Before fixation, cells were stained with Hoechst 33342. Formaldehyde-fixed cells (see below) were incubated with mouse monoclonal anti-FLAG antibody (M2, Sigma) followed by RedX-conjugated goat anti-mouse IgG (Jackson ImmunoResearch Laboratories, West Grove, PA) and examined by epifluorescence microscopy (Zeiss Axioplan microscope; 40× objective, 1.3).

Short interfering RNA (siRNA) transfection. Double-stranded siRNA targeting human ATG5, ATG7 and ATG12 were purchased from Invitrogen (Carlsbad, CA). HepG2 cells were transfected with ATG siRNAs with Metafectene reagent according to manufacturer's instructions (Biontex Laboratories, Germany). In brief, 80 nM siRNA and Metafectene reagent was mixed with Opti-MEM I reduced serum medium and incubated for 20 min at ambient temperature. Afterwards, the mixture was added to freshly trypsinized HepG2 cells (2×10^5) in serum-free medium and incubated 5 h before addition of 10% FBS. At 48 h post transfection, cells were used for pulse-chase experiments or Western blotting.

RT-PCR. Cellular mRNA was isolated using a First Strand cDNA Synthesis kit (Roche) according to the manufacturer's instructions. Serial dilutions of cDNAs were subjected to PCR amplification of EDEM1. GAPDH and actin served as internal standards. PCR products were resolved in 1% agarose gels.

Pulse chase and immunoprecipitation. Cells grown to 70–80% confluency were fed with fresh medium 16 h before metabolic labeling. In the pulse-chase experiments, cells were rinsed quickly once in methionine- and cysteine-free MEM (Sigma), pulsed for 20 min with [^{35}S]methionine-cysteine (120 μCi/ml; NEN, Boston, MA) in methionine- and cysteine-free MEM, washed four times in complete medium and

chased in complete medium supplemented with 4 mM of both methionine and cysteine. For proteasome inhibition, cells were chased in the presence of 1 μM epoxomycin (Sigma), 20 μM MG 132 (Calbiochem, San Diego, CA) or 100 μM ALLN (Calbiochem); for autophagosome accumulation, in the presence of 50 μM vinblastine (Sigma); for inhibition of autophagosome formation with 10 mM 3-methyladenin (Sigma); and for lysosomal protease inhibition in the presence of 10 μg/ml of pepstatin A and E64d (Sigma). For preparation of cell lysates, cells were mechanically removed, centrifuged and resuspended in lysis buffer [10 mM phosphate buffer, pH 7.4, containing 1% Triton X-100 and protease inhibitor cocktail (Roche Diagnostics)] for 30 min on ice. For immunoprecipitation of endogenous EDEM1, lysates were incubated overnight at 4°C with protein A-Dynal magnetic beads (Invitrogen, Dynal AS, Oslo, Norway) precoated with Fc-fragment-specific affinity-purified rabbit anti-goat IgG (Jackson ImmunoResearch Laboratories) and goat anti-human EDEM1 antibody (C-19, Santa Cruz Biotechnology, Santa Cruz, CA). Immunoprecipitates were washed four times with PBS containing 0.5% Triton X-100, boiled in Laemmli buffer for 5 min, resolved by SDS-PAGE and subjected to autoradiography. Densitometric quantification of EDEM1 bands was performed using Image Quant TL software (GE Healthcare, Bio-Science) or ImageJ 1.38r (http://rsb.info.nih.gov/ij). Percentage of degradation was determined in at least four independent experiments. Mean values and standard deviation were calculated using MS Excel. Standard errors $_{(n\text{-}1)}$ of the mean are shown by bars.

Peptide:*N*-glycosidase F digestion. Cell extracts or immunoprecipitated EDEM1 were equilibrated in PNGase F buffer (50 mM Tris, pH 8, 1% Triton X-100) and subjected to deglycosylation by PNGase F (Roche diagnostics, 10 U/ml) for 2 h at 37°C.

Western blot. Cells were harvested and lysed in lysis buffer (PBS) containing 1% Triton X-100 and protease inhibitor cocktail (Roche Diagnostics). After 30-min incubation on ice, cells were centrifuged at 10 000 *g* for 10 min. The supernatant containing Triton X-100-soluble proteins was collected and the pellet containing Triton X-100-insoluble proteins was washed in cold PBS and dissolved by sonication in Laemmli buffer containing 8 M urea. Samples were boiled for 8 min, 1:10 of Triton X-100-soluble and 1:3 of Triton X-100-insoluble fractions were loaded and resolved by SDS-PAGE. Proteins were blotted onto a nitrocellulose membrane. After blocking in 5% Top Block (Fluka, Buchs, Switzerland) or 5% non-fat dry milk in TBS-Tween (20 mM Tris-HCl, pH 7.4, 0.5 M NaCl, 0.1% Tween 20), membranes were analyzed for different proteins. The following primary antibodies were used: goat anti-human EDEM1 peptide antibody (Santa Cruz, C19, sc-27391; N16, sc-27389, both 300-fold diluted), goat anti-human LC3 antibody (Santa Cruz, N20, sc-16755, 1:300), rabbit anti-ATG5 antibody (Cell Signaling Technology Inc., 2630, 1:2000), mouse anti-LAMP1 antibody (RDI Research Diagnostics, Concord, MA, MCD107) and rabbit anti-calnexin antibody (Stressgen Bioreagent, SPA-865, 1:2000). After overnight incubation at 4°C, each blot was probed with horseradish peroxidase (HRP)-conjugated appropriate secondary antibodies (Jackson ImmunoResearch Laboratories, 1:30 000). Immunoreactive bands were visualized by an ECL system (GE Healthcare, Bio-Science).

2-D electrophoresis. IPG strips (Immobiline DryStrip pH 5.3–6.5, GE Healthcare, Sweden) were rehydrated with rehydration buffer (8 M urea, 2% CHAPS, 2% IPG-buffer, 20 mM DTT) overnight at ambient temperature. Immunoprecipitated ^{35}S-labeled EDEM1 was PNGase F digested (see above) and concentrated in Microcon 30 (Millipore, Billerica, MA). Protein samples were mixed with sample preparation buffer (8 M urea, 4% CHAPS, 2% IPG buffer, 40 mM DTT) and applied at the cathodic end onto the strips. Isoelectric focusing was performed using a Multiphore II system (Pharmacia Biothec, Uppsala, Sweden) according to the manufacturer's instructions (300 V for 10 min, 300 V for 6 h, 3500 V for 8 h, 3500 V for 18 h). Afterwards, the IPG strips were incubated in equilibration buffer (8 M urea, 75 mM Tris-HCl pH 8.8, 2% SDS, 0.02% bromophenol blue, 30% glycerol) supplemented with DTT (1% w/v) for 15 min followed by equilibration buffer supplemented with iodoacetamide (2.5% w/v) for 15 min, at ambient temperature. Proteins were then resolved by 8% SDS-PAGE in the second dimension and dried gels were subjected to autoradiography.

OptiPrep density gradient flotation. Post-nuclear supernatants from vinblastine-treated cells were prepared by centrifugation (1000 *g*, 10 min, 4°C) of homogenates (prepared using aTeflon glass homogenizer in 10 mM HEPES pH 7.5 containing 250 mM sucrose, 1 mM EDTA and protease inhibitor cocktail). Supernatant was equilibrated to 35% iodixanol (OptiPrep, Sigma), overlaid with 25% OptiPrep solution and covered with homogenization buffer. After centrifugation (180 000 *g*, 3 h at 4°C), the microsomal fraction was collected at the OptiPrep-buffer interface, equilibrated to 35% iodixanol solution and layered below a 0–30% continuous OptiPrep gradient. The gradients were centrifuged in a

swinging bucket rotor (50 000 *g* for 18 h at 4°C) and fractions collected. Proteins were resolved by SDS-PAGE (6–18%), transferred to nitrocellulose membranes and incubated with antibodies against calnexin (BD Biosciences, Erembodegem, Belgium), LAMP1 (Research Diagnostics Inc., Flanders, NJ), EDEM1 (C-19), and LC3 (N20) overnight at 4°C followed by HRP-conjugated secondary antibodies and visualization by ECL.

Immuno-purification of autophagosomes. Microsomal fraction of vinblastine-treated cells was prepared as described above and equilibrated with PBS containing 1 mM EDTA, 0.2% BSA and protease inhibitor cocktail. Autophagosomes were immuno-purified with either rabbit anti-human LC3 antibodies (H50) or goat anti-human LC3 antibodies (N20) covalently dithiobis(succinimidyl propionate) (DSP)-cross-linked to protein A-Dynal magnetic beads. As control, non-immune rabbit or goat serum was covalently DSP-cross-linked to the beads. The immunoprecipitates were boiled in Laemmli buffer, resolved by SDS-PAGE (6–18%) and analyzed for EDEM1 or LC3 by Western blot (see above).

Immunofluorescence. Cells were grown on coverslips to 60–70% confluency and fed with fresh medium 16 h before fixation. Formaldehyde fixation and saponin permeabilization as well as antibody incubations were performed as previously reported [14]. For single, double and triple immunolabeling goat anti-human EDEM1, rabbit anti-LC3 (H50) and mouse monoclonal anti-human LAMP1 (Research Diagnostics Inc.) antibodies were applied followed by fluorescent, not cross-reactive, secondary antibodies. Immunofluorescence was recorded with Leica confocal laser scanning microscopes SP2 or SP5 (Leica, Wetzlar, Germany) using the 100× objective (1.4). In double- and triple-immunofluorescence overlays, effects of z-axis pixel shifts were corrected.

Immunoelectron microscopy. Cells grown to near confluency were double aldehyde-fixed as described [14]. Frozen ultrathin sections were prepared according to Tokuyasu and immunogold-labeled for EDEM1 as described [14].

Pre-embedding immunoperoxidase labeling for EDEM1 was performed as described [14] and serial ultrathin sections were prepared in the plane of the cell layer.

Results

Overexpression of EDEM1 can be deleterious to cultured cells. Our previous work [14] has shown that endogenous EDEM1 in different mammalian cell types is restricted inside the ER to portions of a few cisternae. This unexpected observation indicates that protein levels of EDEM1 in the ER are tightly regulated and that its uncontrolled overexpression may be deleterious to cells. To test this, HepG2, HeLa and HEK293 cells were simultaneously transfected with EDEM1-FLAG under the control of a CMV promoter and with EGFP targeted to the Golgi apparatus by the cytosolic domain of endomannosidase as transfection reporter protein (C1-rat endomannosidase-EGFP; see [32]). Although about 20% of HepG2 cells expressed EDEM1-FLAG/Golgi-EGFP after a 5-h transfection period, the EDEM1-FLAG/Golgi-EGFP-expressing cells observed after 1 day were non-colony-forming, single cells (Fig. 1A). Following 3 or 7 days in culture, the few remaining EDEM1-FLAG/Golgi-EGFP-expressing cells were non-colony-forming giant cells (Fig. 1B, C). The HeLa cells expressing EDEM1-FLAG/Golgi-EGFP were rounded and exhibited fragmented nuclei, although more cells survived after 7 days in culture compared to EDEM1-transfected HepG2 cells (Fig. 1D–F). As in the case of HepG2 cells, the EDEM1-FLAG/Golgi-EGFP-expressing HeLa cells were only single, non-colony-forming cells. The controls, HepG2 and HeLa cells transfected with p3xFLAG-CMV vector/Golgi-EGFP showed no signs of cytotoxicity up to 7 days after transfection (Supplementary Fig. 1). HEK293 cells were least sensitive to EDEM1 overexpression since, at 7 days after transfection, EDEM1-expressing cells were observed (Fig. 1G–I). In agreement with this observation, another group reported that EDEM1 overexpression is not deleterious to HEK293 cells and actually protects them against the action of ricin [10]. By semiquantitative RT-PCR, control HEK293 cells contained about four times less EDEM1 mRNA compared with HepG2 cells (Supplementary Fig. 2), which may explain the differential sensitivity of these cell lines to EDEM1 overexpression. Taken together, uncontrolled expression of EDEM1 over a certain level resulted in deleterious effects that blocked cell division and caused apoptotic cell death in the cell lines studied.

Influence of proteasome inhibition on degradation of endogenous EDEM1. To clarify the role of proteasomes in the degradation of endogenous EDEM1, HepG2 cells were metabolically labeled with [^{35}S]cysteine/methionine and chased in the presence

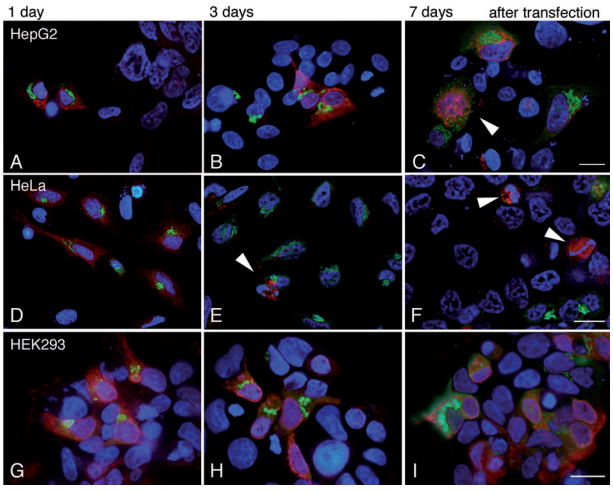

Figure 1. Overexpression of EDEM1 results in cytotoxicity. HepG2 cells (*A–C*), HeLa cells (*D–F*) and HEK293 cells (*G–I*) were simultaneously transiently transfected to express EDEM1-FLAG (red) and as reporter protein Golgi-targeted EGFP (green). In all cell types, overexpressed EDEM1 (red) is distributed throughout the cytoplasm, and in HepG2 cells results in giant cell formation (*C*), and in HeLa cells in fragmentation of nuclei as indication of apoptosis (*E, F*). HEK293 cells overexpressing EDEM1 (*G-I*) as well as HepG2 and HeLa cells expressing only Golgi-EGFP show undisturbed morphology. Nuclei are stained in blue by Hoechst 33342. Bars, 10 μm.

of various proteasome inhibitors (Fig. 2). All pulse-chase experiments were performed under non-starvation conditions to prevent unwanted starvation effects such as induced proteasomal protein degradation [33] or blockage of eIF4-dependent protein synthesis by the induction of an unfolded protein response [34]. Clearance rates of proteins in pulse-chase experiments can be accurately measured by the estimation of the slope of the degradation curve. The estimation of the residual relative amount of the proteins present at a given time and the calculation of half-lives are not as reliable. Therefore, we calculated the EDEM1 clearance rate per hour from at least three independent experiments. The affinity-purified anti-EDEM1 peptide antibodies used in our experiments reacted with both glycosylated and deglycosylated forms of EDEM1 with the expected molecular masses in Western blots (Supplementary Fig. 3A). At the end of a 30-min pulse, heterogeneously glycosylated forms of EDEM1 (based on PNGase F sensitivity, Supplementary Fig. 3B) and one not glycosylated EDEM1 form were immunoprecipitated (Fig. 2A), as previously observed in translation experiments *in vitro* using a different EDEM1-specific antibody (Fig. 1B in [14]). The immunoprecipitated and PNGase F deglycosylated EDEM1 from HepG2 cell lysates migrated in 2-D gels at the calculated isoelectric points at 6.2 (asparagine form of EDEM1) and 5.8 (deglycosylated, aspartate form of EDEM1) (Supplementary Fig. 3C). Treatment with the proteasome inhibitors epoxomycin or MG 132 (Fig. 2) as well as ALLN (not shown) did not inhibit the clearance of glycosylated EDEM1 and only marginally inhibited clearance of deglycosylated EDEM1 during the second hour of chase (Fig. 2C). Actually, proteasome inhibition seemed to enhance the clearing of glycosylated EDEM1 during the first hour of chase (Fig. 2C). In our experiments, we had to allow for the fact that the rate of disappearance of the glycosylated EDEM1 reflects its rate of de-glycosylation. This explains the higher percentage of clearance of deglycosylated EDEM1 observed after 2-h treatment with proteasome inhibitors as compared to 1-h treatment (Fig. 2C). In accordance, and in contrast to vinblastine (see below), proteasome inhibitors did not affect the clearance of intermediate glycosylated EDEM1 (Fig. 2C). The effectiveness of the proteasome inhibitors used in our experiments was verified simultaneously by Western blot for polyubiquitin. Accumulation of polyubiquitinated proteins was already significant after 1 h of treatment with proteasomal inhibitors (Supplementary Fig. 4) and remained high during the entire time period of proteasome inhibition, as expected [35, 36]. Together, these data demonstrated that the proteasome inhibitors used did not stabilize endogenous EDEM1, indicating the existence of another degradation pathway.

EDEM1 is degraded by autophagy. To explore the possibility that autophagy is involved in the degradation of EDEM1, we used LC3A, the LC3 paralog highly expressed in hepatocytes (http://www.uniprot.org/uniprot/Q9H492), as specific autophagosome membrane marker [35, 36]. We observed endogenous EDEM1 in autophagosomes of HepG2 cells under basal conditions by double confocal immunofluorescence for endogenous LC3A and EDEM1 (Fig. 3A–F, inset 1) and by immunogold electron microscopy (Fig. 3G). In addition, we observed EDEM1 in LC3A- and LAMP1-positive structures corresponding to autophagolysosomes (Fig. 3A–F, inset 2) as well as in LC3A-negative but LAMP1-positive structures that correspond to lysosomes (Fig. 3A–F, inset 3). Clearance of cytosolic proteins by autophagy has been shown to correlate with their propensity to aggregate [37–39]. We obtained evidence compatible with the presence of aggregated cytosolic EDEM1 by detecting both Triton X-100-soluble and Triton X-100-insoluble EDEM1 (Fig. 4A). Of note, the Triton X-100-insoluble EDEM1 was deglycosylated. Furthermore, by immunoelectron microscopy, clusters of EDEM1 were observed that were partially or completely surrounded by double-membrane structures typical of forming and of mature autophagosomes,

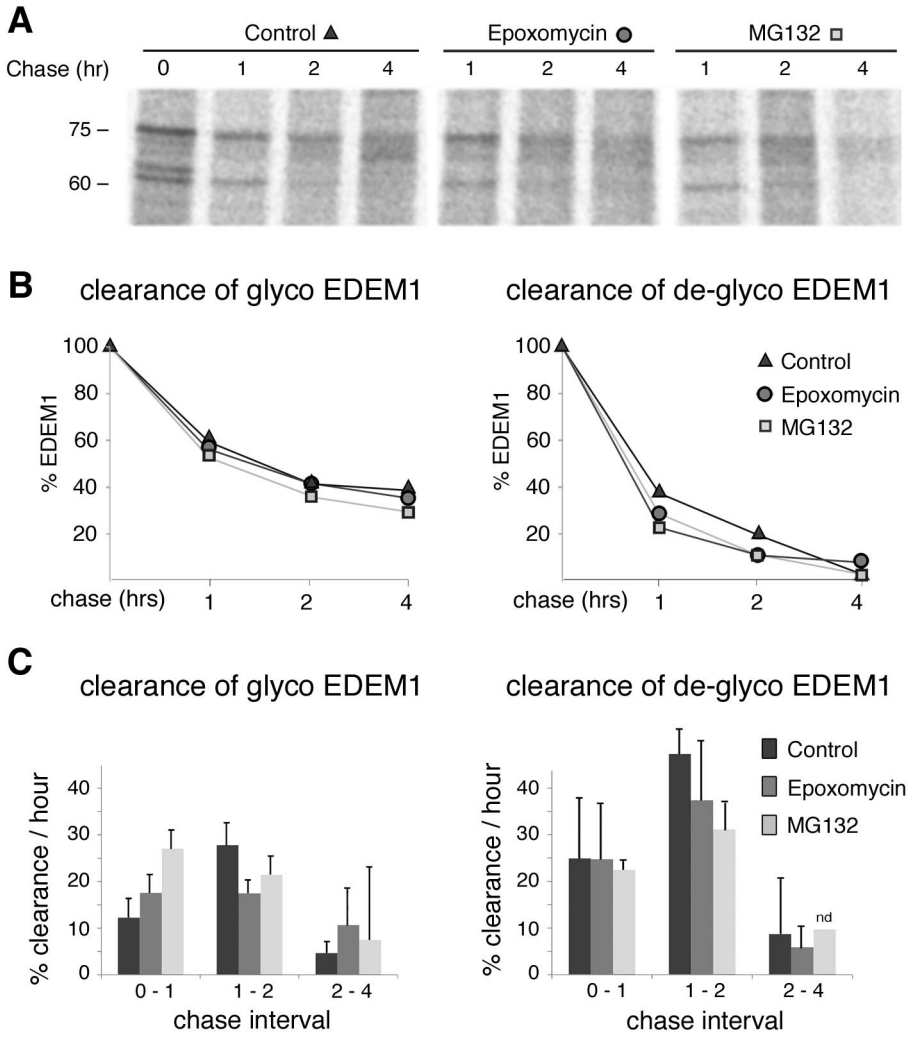

Figure 2. Endogenous EDEM1 is not degraded by proteasomes. (*A*) Non-starved HepG2 cells were pulsed for 20 min with [^{35}S]cysteine/methionine and chased for the indicated times in the absence (control) or presence of epoxomycin or MG132. Immunoprecipitates prepared from post-nuclear fractions of cell lysates with anti-EDEM1 antibodies were resolved by reducing SDS-PAGE and subjected to autoradiography. (*B*) Densitometry of residual EDEM1 at different chase time points of the experiment shown in (*A*) is presented. (*C*) Clearance rate (percentage of EDEM1 removed per hour) of glycosylated (left) and deglycosylated (right) EDEM1 was obtained from three independent experiments and its mean is shown (glyco, glycosylated, deglyco, deglycosylated). Bars represent standard error of the mean.

respectively (Figs. 4B and 3G), providing further evidence of autophagy of cytosolic EDEM1 aggregates.

Since the actual number of autophagosomes under basal conditions is rather small in mammalian cells, HepG2 cells were treated with vinblastine to block their fusion with lysosomes and to increase their number [40, 41]. By triple confocal immunofluorescence (Fig. 5A–D), we then observed numerous LC3-positive structures throughout the cytoplasm (Fig. 5B) and co-distribution of EDEM1 with numerous autophagosomes (Fig. 5C, D). By serial section immunoperoxidase electron microscopy, groups of EDEM1-containing typical autophagosomes were observed in vinblastine-treated HepG2 cells (Fig. 5E, F and Supplementary Fig. 5). In the same cells, both EDEM1-positive autophagosomes (AP1 and AP2 in Fig. 5F) and EDEM1-unreactive autophagosomes, which contained fragments of ER profiles (AP3 in Fig. 5F), were noticed by immunoelectron microscopy. As an indication of successful inhibition of autophagosome-lysosome fusion, vinblastine treatment in pulse-chase experiments resulted in an increase of the autophagosome membrane-anchored LC3A-II form (Supplementary Fig. 6).

The presence of EDEM1 in autophagosomes was independently verified biochemically by the detection of EDEM1 immunoreactivity in LC3A immunopurified vesicles obtained from post-nuclear microsomal fractions (Fig. 5G). The sole LC3A form detected in these purified vesicles was, as to be expected [35], the membrane-bound LC3A-II form. In OptiPrep gradients, immunoreactivity of glycosylated and deglycosylated EDEM1 co-migrated with LC3A-I, LC3A-II and LAMP1 membranes in light-density fractions (Fig. 5H, fractions 2, 3). They were separate from denser, calnexin-immunoreactive fractions, containing ER membranes (Fig. 5H, fractions $\geq$4). The major EDEM1-containing light-density fraction was associated with the autophagosome

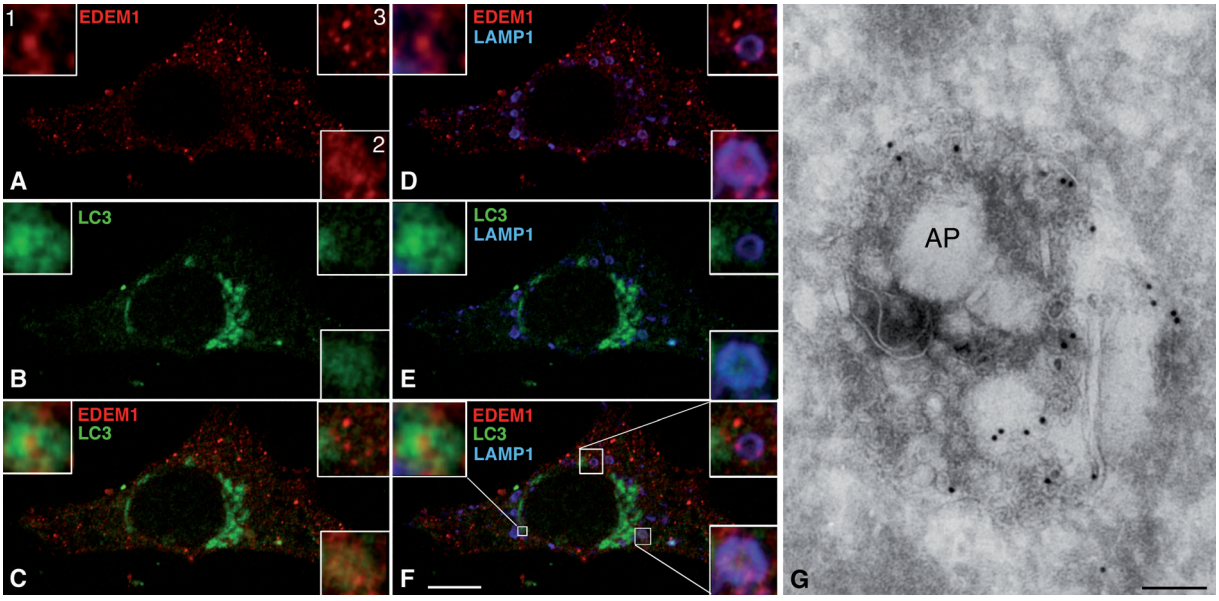

Figure 3. Endogenous EDEM1 is detected in autophagosomes. (*A–F*) HepG2 cells were triple labeled for endogenous EDEM1, endogenous LC3 as marker for autophagosome membrane and endogenous LAMP1 as marker for lysosomes and analyzed by confocal immunofluorescence microscopy. A single optical section through a HepG2 cell is shown. Higher magnification insets (1–3) show examples of localization of EDEM1 in autophagosomes (insets 1), in phagolysosomes (insets 2), or in lysosomes (insets 3). Bar, 10 μm. (*G*) Ultrathin frozen sections of HepG2 cells were immunogold-labeled for endogenous EDEM1 and show its presence in an autophagosome (AP) with the typical double membrane. Bar, 125 nm.

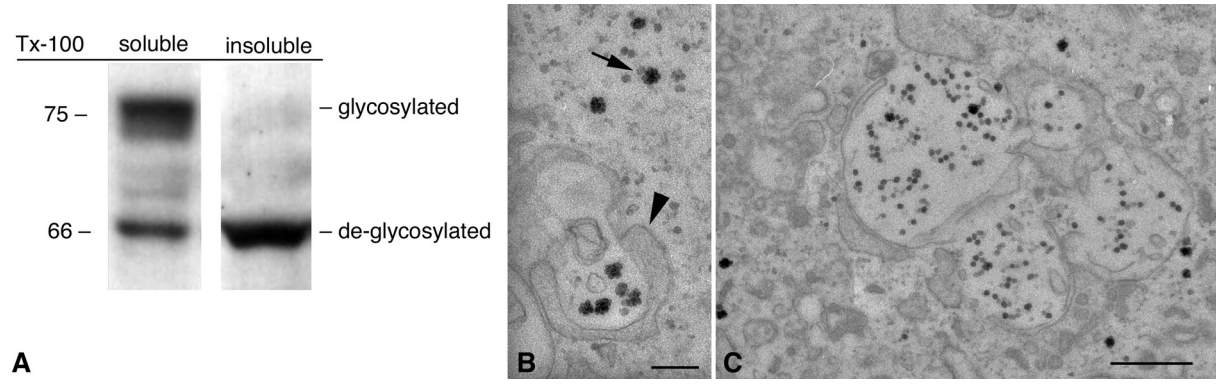

Figure 4. Endogenous EDEM1 is found in aggregates and delivered to autophagosomes. (*A*) By Western blot, EDEM1 is detected in Triton X-100-soluble and -insoluble fractions of HepG2 cells. Both glycosylated and deglycosylated EDEM1 is detected in the Triton X-100-soluble fraction, whereas only deglycosylated EDEM1 is detectable in Triton X-100-insoluble fraction. For the analysis of the insoluble fraction, three times as much material as for the soluble fraction was loaded. (*B, C*) EDEM1 immunolabeling is detected in HepG2 cells as clusters in the cytosol (arrow in *B*). Such clusters are partially (arrowhead in B) or completely surrounded by double membranes typical of autophagosomes. Bars, 300 nm (*A*); 1 μm (*B*).

membrane marker LC3A-II. It is therefore different from the very dense EDEM1-containing fraction that co-migrated with the insoluble, tubulin-associated LC3-I form reported by others [17].

Next, the influence of vinblastine treatment on the clearance of EDEM1 glyco-forms was analyzed in pulse-chase experiments (Fig. 6). Vinblastine, but not pepstatin/E64d, slightly delayed the clearance of the glycosylated EDEM1 (Fig. 6A–C). De-glycosylation of EDEM1 was delayed under vinblastine for about 1 h, as shown by the stabilization effect on the intermediate glycosylated forms (arrowheads in Fig. 6A). However, vinblastine had an immediate strong inhibitory effect on the clearance of deglycosylated EDEM1 (Fig. 6A–C). This stabilization effect lasted for about 2 h. The effect of combined pepstatin A/E64d treatment, inhibitors of major lysosomal aspartic and cysteine proteases [42], on EDEM1 did not last as long, probably due to the activities of other lysosomal hydrolases. It delayed the clearance of the deglycosylated EDEM1 during the first hour of chase but not of the glycosylated one (Fig. 6A–C).

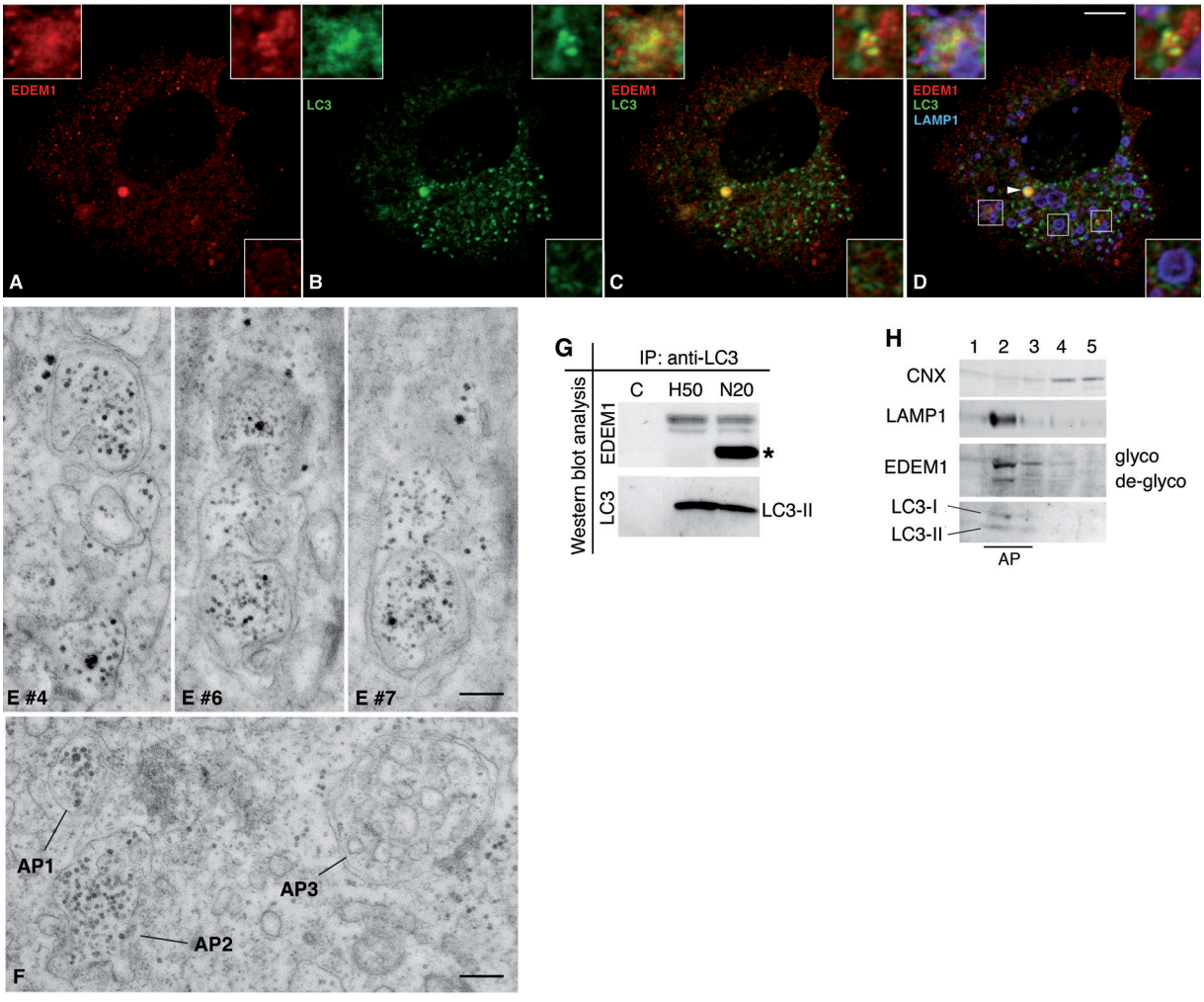

Figure 5. Endogenous EDEM1 is degraded by autophagy. (*A – D*) HepG2 cells were treated with vinblastine to enrich for autophagosomes. Triple confocal immunofluorescence labeling for endogenous EDEM1, endogenous LC3 and endogenous LAMP1. A single optical section through a HepG2 cell is shown. The insets illustrate the distribution of the three proteins at higher magnification and their distribution relative to each other is shown in the overlay (*D*). Arrowhead in (*D*) points to a residual body. Bar, 10 μm. (*E*) Immunoperoxidase pre-embedding labeling for EDEM1 in vinblastine-treated (30 min) HepG2 cells. Three serial ultrathin sections (#4, #6, #7) out of a larger series (see Supplementary Fig. 5) demonstrate EDEM1 in a group of typical autophagosomes. Bar, 400 nm. (*F*) Three autophagosomes are shown, two of which are positive for EDEM1 (AP1 and AP2). The autophagosome (AP3) containing ER profiles is not labeled for EDEM1. Bar, 300 nm. (*G*) Autophagosomes were immuno-purified with LC3 antibody-coated magnetobeads from vinblastine-treated HepG2 cells, resolved by reducing SDS-PAGE and subjected to Western blot analysis for EDEM1 or LC3. Asterisk indicates heavy chain of homologue Ig. (*H*) Post-nuclear cellular membranes from vinblastine-treated HepG2 cells were separated in a continuous 0–30% OptiPrep gradient. Fractions in the order of increasing density were resolved on reducing SDS-PAGE and probed for calnexin (CNX), LAMP1, EDEM1 and LC3. AP, Fractions containing autophagosomes/phagolysosomes.

Autophagosome formation can be inhibited either by 3-methyladenine [43] or by siRNA-mediated knock-down of ATG5, ATG7, and ATG12 [28]. 3-Methyl-adenine treatment stabilized the deglycosylated form of EDEM1 (Supplementary Fig. 7A). Simultaneous transfection of HepG2 cells with siRNAs for ATG5, ATG7 and ATG12 for 48 h efficiently blocked the formation of autophagosomes as indicated by the lack of ATG5-ATG12 complexes and an increased amount of the cytosolic form of LC3A-I (Fig. 6D). This resulted in the accumulation of deglycosylated EDEM1 in the Triton X-100-insoluble fraction, indicating its aggregated state (Fig. 6D). Triton X-100-insoluble EDEM1 was also observed in cells under steady-state conditions (see Fig. 4A). In the Triton X-100-soluble fraction, both glycosylated and deglycosylated EDEM1 was found (Fig. 6D). Taken together, both morphological and biochemical analysis indicated that endogenous EDEM1 under normal conditions was degraded by basal autophagy.

Since we had previously observed EDEM1 in limited portions of single ER cisternae [14], a serial section analysis was performed to clarify whether these EDEM1-containing ER cisternae were removed by

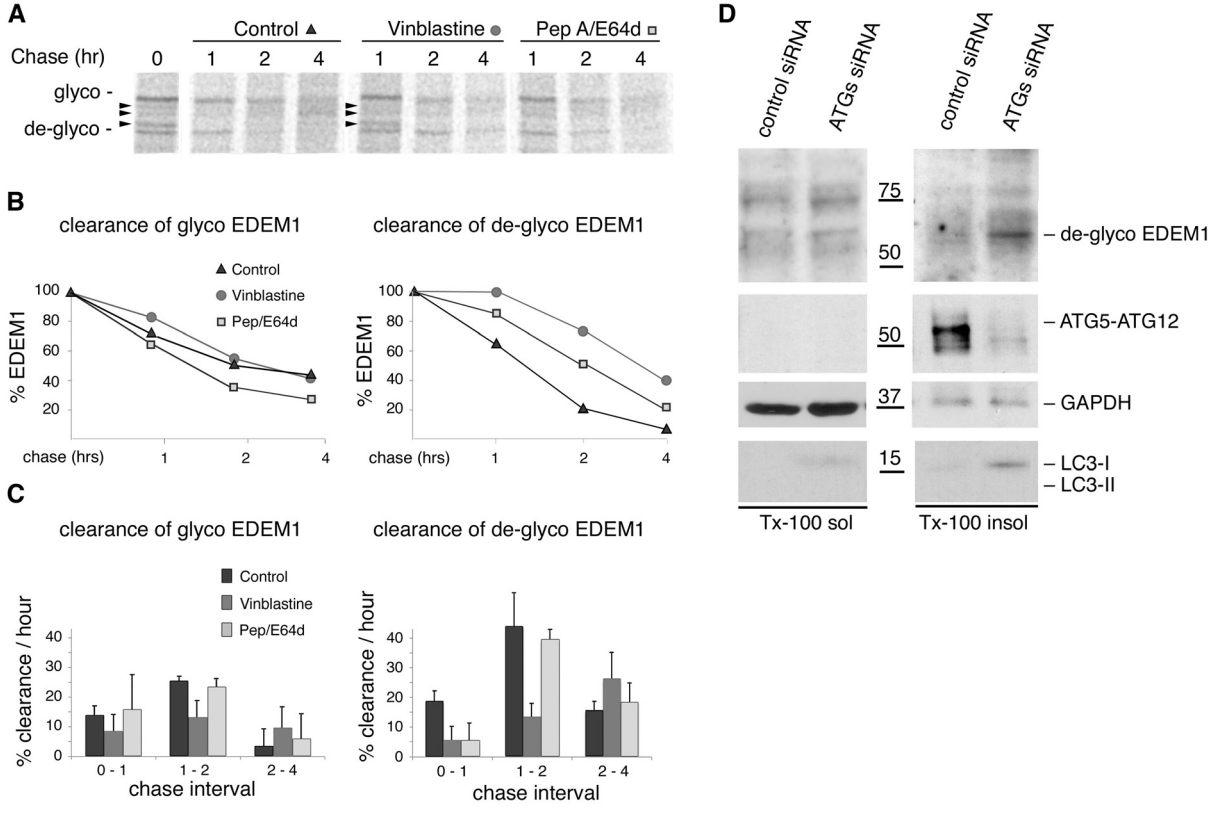

Figure 6. Endogenous EDEM1 is degraded by autophagy. (*A*) HepG2 cells were pulsed for 20 min with ^{35}S-labeled methionine/cysteine and chased for the indicated times in the absence (control) or presence of vinblastine or pepstatin A/E64d. Cell lysates were immunoprecipitated with anti-EDEM1 antibodies, resolved by reducing SDS-PAGE and subjected to autoradiography. (*B*) Densitometry of residual EDEM1 at different chase time points of the experiment shown in (*A*) is presented. (*C*) Clearance rate (percentage of EDEM1 removed per hour) of glycosylated (left) and deglycosylated (right) EDEM1 was obtained from three independent experiments and its mean is shown. Bars represent standard error of the mean. (*D*) HepG2 cells were incubated with siRNA targeting mRNAs of ATG5, ATG7, and ATG12 for 48 h. Western blot analysis for EDEM1, ATG5-ATG12 complexes, GAPDH and LC3 of cell lysates from Triton X-100-soluble and -insoluble fractions is shown. As control, siRNA of α1-antitrypsin was used since this secretory protein is abundant in HepG2 cells.

autophagy. However, EDEM1-containing ER was not observed in autophagosomes and, *vice-versa*, EDEM1-positive autophagosomes did not contain ER profiles (Fig. 7). This is in agreement of the clearance of cytosolic EDEM1 clusters by autophagy (Fig. 4B).

Discussion

The degradation pathway of ERAD substrates is well known [3, 4], in contrast to the pathway taken by machinery proteins of the protein quality control. In the present study, we aimed to determine the degradation pathway of the ERAD component EDEM1 under basal conditions in cells not stressed by the overexpression of a transgenic misfolded glycoprotein. We observed that endogenous EDEM1 after exit from the ER becomes deglycosylated, forms cytosolic aggregates and is degraded by basal autophagy. Furthermore, we obtained evidence that keeping EDEM1 protein at endogenous levels is of physiological importance, since uncontrolled overexpression of EDEM1 evoked cytotoxic effects.

Our data show that overexpression of EDEM1 can exert cytotoxic effects in cells not stressed by starvation or by an overload with transgenic ERAD substrates. Although the mechanism leading to EDEM1 cytotoxicity is unclear at present, we propose that the surplus of EDEM1 cannot be efficiently removed by the steady-state ER-clearance mechanism for EDEM1 [14]. The surplus EDEM1 present throughout the ER is fully functional, as shown by the accelerated release of overexpressed ERAD substrates from calnexin and their clearance [8, 9]. However, in normal cells, this may result in an indiscriminatory interaction of EDEM1 with all kind of glycoproteins carrying mannose-trimmed *N*-glycans and their retention in the ER lumen.

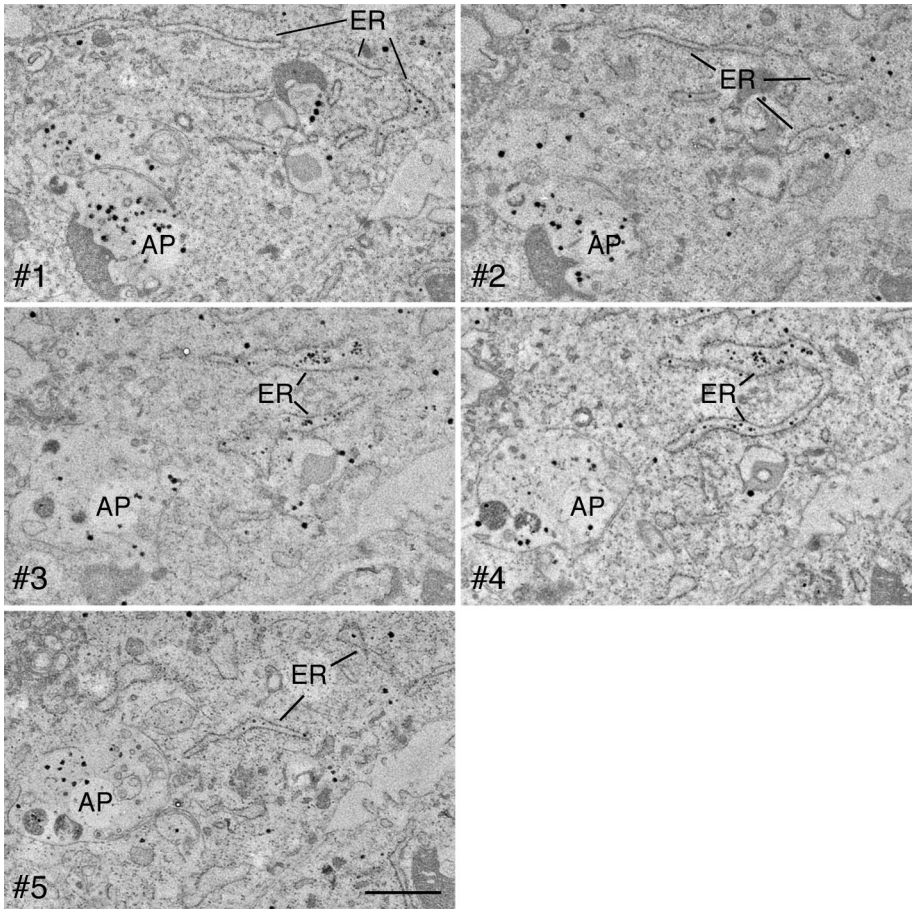

Figure 7. EDEM1 containing ER cisternae are not subjected to ER-phagy. Pre-embedding immunoperoxidase immunolabeling for EDEM1. In this series of consecutive ultrathin sections, an EDEM1-labeled ER cisterna (ER), which can be followed through all sections and a nearby EDEM1-labeled autophagosome (AP) are observed. Bar, 850 nm.

None of the proteasome inhibitors used in our experiments delayed the turnover of EDEM1, similar to that reported for mouse fibroblasts treated with the proteasome inhibitor PS-341 [17]. At least two possible mechanisms can be envisaged in explanation. We favor that EDEM1 is genuinely degraded by autophagy since the inhibitors of the autophagy-lysosome pathway acted not only efficiently but also rapidly. Alternatively, proteasomal degradation could be the inherent pathway of EDEM1 and its functional blockade could be compensated for by autophagy. However, we believe this not to be likely, since, in ATG siRNA knockdown experiments combined with proteasome inhibition by MG 132, no surplus Triton X-100-insoluble EDEM1 was detected (Supplementary Fig. 7). We noticed that under the various conditions applied for autophagy-lysosome inhibition, EDEM1 was not fully stabilized. In fact, about 50 % was lost during the chase. This was due to the formation of Triton X-100-insoluble cytosolic EDEM1 aggregates. In agreement, EDEM1 aggregates were detected in LC3-I-containing high-density fractions of mouse embryonic fibroblasts [17]. Such EDEM1-containing aggregates could not be immunoprecipitated since they were contained in the nuclear fraction (unpublished data). This is probably also the reason why EDEM1 became undetectable in ATG5$^{-/-}$ cells [17]. The question then arises why the EDEM1-containing aggregates are not deleterious in autophagy-incompetent cells. In this regard, it has been shown that accumulated protein aggregates become distributed asymmetrically during mitosis to one daughter cell, leaving the other free of accumulated aggregates [44]. This would explain why autophagy-incompetent cells like ATG5$^{-/-}$ cells can survive in culture.

The majority of endogenous EDEM1 is found outside the lumen of the ER under basal conditions and only limited portions of a few ER cisternae contain EDEM1 [14]. In the present electron microscopic serial section analysis, no evidence for autophagic removal of EDEM1-containing parts of the ER was found. Thus, autophagy of EDEM1 comprises the clearance of cytosolic EDEM1 aggregates and has to be distinguished from the autophagy of ER cisternae containing aggregated misfolded protein [45, 46], or from ER-phagy, which is the selective autophagy of surplus ER under non-steady state conditions [31, 47, 48]. There is other evidence that the autophagy-lysosome system, but not proteasomes, are involved in

the degradation of proteins of the ER protein quality control machinery. For instance, ER glucosidase II was detected in autophagosomes [49], which seems to be its degradation pathway [50]. Furthermore, degradation of ER mannosidase I did not occur by proteasomes but through lysosomal enzymes [51].

Proteins present in the cytosol may not become degraded by proteasomes for simple sterical reason since they must be unfolded before they can be translocated into the proteolytic core of the proteasome [52]. As a case in point, aggregate-prone cytosolic proteins, which are a hallmark of chronic neurodegenerative diseases, have been shown to be preferentially degraded by autophagy [37–39]. Moreover, it has been shown that surplus single fibrinogen chains are degraded by proteasomes, whereas surplus dimeric fibrinogen chains are not [53–55]. EDEM1, which exits the ER by a vesicular pathway [14], apparently becomes deglycosylated in the cytosol and forms detergent-insoluble aggregates. Further studies are required to determine whether or not this takes place in complex with the bound substrate. Likewise, additional studies are needed to uncover the mechanism by which EDEM1 becomes cytosolic and if the membrane of the EDEM1 vesicles has to be disintegrated for this mechanism [56, 57].

In conclusion, our data demonstrate that endogenous EDEM1 after its exit from the ER lumen is degraded by basal autophagy. The present results also suggest that EDEM1 is not recycled but undergoes degradation similar as the ERAD substrates themselves.

Electronic supplementary material. Supplementary material is available in the online version of this article at springerlink.com (DOI 10.1007/s00018-009-9038-1) and is accessible for authorized users.

Acknowledgments. We thank Tamara Locher for skilful technical assistance. This work was supported by the Swiss National Science Foundation and the Canton of Zurich.

1 Ellgaard, L. and Helenius, A. (2003) Quality control in the endoplasmic reticulum. Nat. Rev. Mol. Cell Biol. 4, 181–91.
2 Roth, J., Yam, G. H., Fan, J., Hirano, K., Gaplovska-Kysela, K., Le Fourn, V., Guhl, B., Santimaria, R., Torossi, T., Ziak, M. and Zuber, C. (2008) Protein quality control: The who's who, the where's and therapeutic escapes. Histochem. Cell Biol. 129, 163–77.
3 Hiller, M. M., Finger, A., Schweiger, M. and Wolf, D. H. (1996) ER degradation of a misfolded luminal protein by the cytosolic ubiquitin-proteasome pathway. Science 273, 1725–8.
4 Meusser, B., Hirsch, C., Jarosch, E. and Sommer, T. (2005) ERAD: The long road to destruction. Nat. Cell Biol. 7, 766–72.
5 Jakob, C. A., Bodmer, D., Spirig, U., Battig, P., Marcil, A., Dignard, D., Bergeron, J. J., Thomas, D. Y. and Aebi, M. (2001) Htm1p, a mannosidase-like protein, is involved in glycoprotein degradation in yeast. EMBO Rep. 2, 423–30.
6 Hosokawa, N., Wada, I., Hasegawa, K., Yorihuzi, T., Tremblay, L. O., Herscovics, A. and Nagata, K. (2001) A novel ER alpha-mannosidase-like protein accelerates ER-associated degradation. EMBO Rep. 2, 415–22.
7 Nakatsukasa, K., Nishikawa, S., Hosokawa, N., Nagata, K. and Endo, T. (2001) Mnl1p, an alpha -mannosidase-like protein in yeast *Saccharomyces cerevisiae*, is required for endoplasmic reticulum-associated degradation of glycoproteins. J. Biol. Chem. 276, 8635–8.
8 Molinari, M., Calanca, V., Galli, C., Lucca, P. and Paganetti, P. (2003) Role of EDEM in the release of misfolded glycoproteins from the calnexin cycle. Science 299, 1397–400.
9 Oda, Y., Hosokawa, N., Wada, I. and Nagata, K. (2003) EDEM as an acceptor of terminally misfolded glycoproteins released from calnexin. Science 299, 1394–7.
10 Slominska-Wojewodzka, M., Gregers, T. F., Walchli, S. and Sandvig, K. (2006) EDEM is involved in retrotranslocation of ricin from the endoplasmic reticulum to the cytosol. Mol. Biol. Cell 17, 1664–75.
11 Oda, Y., Okada, T., Yoshida, H., Kaufman, R. J., Nagata, K. and Mori, K. (2006) Derlin-2 and Derlin-3 are regulated by the mammalian unfolded protein response and are required for ER-associated degradation. J. Cell Biol. 172, 383–93.
12 Lilley, B. N. and Ploegh, H. L. (2004) A membrane protein required for dislocation of misfolded proteins from the ER. Nature 429, 834–40.
13 Ye, Y., Shibata, Y., Yun, C., Ron, D. and Rapoport, T. A. (2004) A membrane protein complex mediates retro-translocation from the ER lumen into the cytosol. Nature 429, 841–7.
14 Zuber, C., Cormier, J. H., Guhl, B., Santimaria, R., Hebert, D. N. and Roth, J. (2007) EDEM1 reveals a quality control vesicular transport pathway out of the endoplasmic reticulum not involving the COPII exit sites. Proc. Natl. Acad. Sci. USA 104, 4407–12.
15 Suzuki, T., Seko, A., Kitajima, K., Inoue, Y. and Inoue, S. (1993) Identification of peptide:*N*-glycanase activity in mammalian derived cultured cells. Biochem. Biophys. Res. Commun. 194, 1124–30.
16 Suzuki, T., Kwofie, M. A. and Lennarz, W. J. (2003) Ngly1, a mouse gene encoding a deglycosylating enzyme implicated in proteasomal degradation: Expression, genomic organization, and chromosomal mapping. Biochem. Biophys. Res. Commun. 304, 326–32.
17 Cali, T., Galli, C., Olivari, S. and Molinari, M. (2008) Segregation and rapid turnover of EDEM1 by an autophagy-like mechanism modulates standard ERAD and folding activities. Biochem. Biophys. Res. Commun. 371, 405–10.
18 Bonifacino, J. S. and Weissman, A. M. (1998) Ubiquitin and the control of protein fate in the secretory and endocytic pathways. Annu. Rev. Cell Dev. Biol. 14, 19–57.
19 Klionsky, D. (2004) Autophagy. Landes Bioscience, Georgetown.
20 Komatsu, M., Waguri, S., Chiba, T., Murata, S., Iwata, J., Tanida, I., Ueno, T., Koike, M., Uchiyama, Y., Kominami, E. and Tanaka, K. (2006) Loss of autophagy in the central nervous system causes neurodegeneration in mice. Nature 441, 880–4.
21 Komatsu, M., Waguri, S., Ueno, T., Iwata, J., Murata, S., Tanida, I., Ezaki, J., Mizushima, N., Ohsumi, Y., Uchiyama, Y., Kominami, E., Tanaka, K. and Chiba, T. (2005) Impairment of starvation-induced and constitutive autophagy in Atg7-deficient mice. J. Cell Biol. 169, 425–34.
22 Hara, T., Nakamura, K., Matsui, M., Yamamoto, A., Nakahara, Y., Suzuki-Migishima, R., Yokoyama, M., Mishima, K., Saito, I., Okano, H. and Mizushima, N. (2006) Suppression of basal autophagy in neural cells causes neurodegenerative disease in mice. Nature 441, 885–9.
23 Mizushima, N. and Klionsky, D. J. (2007) Protein turnover *via* autophagy: Implications for metabolism. Annu. Rev. Nutr. 27, 19–40.
24 Mizushima, N., Levine, B., Cuervo, A. M. and Klionsky, D. J. (2008) Autophagy fights disease through cellular self-digestion. Nature 451, 1069–75.

25 Levine, B. and Deretic, V. (2007) Unveiling the roles of autophagy in innate and adaptive immunity. Nat. Rev. Immunol. 7, 767–77.
26 Maiuri, M. C., Zalckvar, E., Kimchi, A. and Kroemer, G. (2007) Self-eating and self-killing: Crosstalk between autophagy and apoptosis. Nat. Rev. Mol. Cell Biol. 8, 741–52.
27 Juhasz, G., Csikos, G., Sinka, R., Erdelyi, M. and Sass, M. (2003) The *Drosophila* homolog of Aut1 is essential for autophagy and development. FEBS Lett. 543, 154–8.
28 Xie, Z. and Klionsky, D. J. (2007) Autophagosome formation: Core machinery and adaptations. Nat. Cell Biol. 9, 1102–9.
29 Ogata, M., Hino, S., Saito, A., Morikawa, K., Kondo, S., Kanemoto, S., Murakami, T., Taniguchi, M., Tanii, I., Yoshinaga, K., Shiosaka, S., Hammarback, J. A., Urano, F. and Imaizumi, K. (2006) Autophagy is activated for cell survival after endoplasmic reticulum stress. Mol. Cell Biol. 26, 9220–31.
30 Yorimitsu, T., Nair, U., Yang, Z. and Klionsky, D. J. (2006) Endoplasmic reticulum stress triggers autophagy. J. Biol. Chem. 281, 30299–304.
31 Bernales, S., McDonald, K. L. and Walter, P. (2006) Autophagy counterbalances endoplasmic reticulum expansion during the unfolded protein response. PLoS Biol 4, e423.
32 Torossi, T., Roth, J. and Ziak, M. (2007) A single tryptophan residue of endomannosidase is crucial for Golgi localization and *in vivo* activity. Cell. Mol. Life Sci. 64, 1881–9.
33 Vabulas, R. M. and Hartl, F. U. (2005) Protein synthesis upon acute nutrient restriction relies on proteasome function. Science 310, 1960–3.
34 Shang, J., Gao, N., Kaufman, R. J., Ron, D., Harding, H. P. and Lehrman, M. A. (2007) Translation attenuation by PERK balances ER glycoprotein synthesis with lipid-linked oligosaccharide flux. J. Cell Biol. 176, 605–16.
35 Kabeya, Y., Mizushima, N., Ueno, T., Yamamoto, A., Kirisako, T., Noda, T., Kominami, E., Ohsumi, Y. and Yoshimori, T. (2000) LC3, a mammalian homologue of yeast Apg8p, is localized in autophagosome membranes after processing. EMBO J. 19, 5720–8.
36 Uchiyama, Y., Shibata, M., Koike, M., Yoshimura, K. and Sasaki, M. (2008) Autophagy–physiology and pathophysiology. Histochem. Cell Biol 129, 407–20.
37 Ravikumar, B., Duden, R. and Rubinsztein, D. C. (2002) Aggregate-prone proteins with polyglutamine and polyalanine expansions are degraded by autophagy. Hum. Mol. Genet. 11, 1107–17.
38 Verhoef, L. G., Lindsten, K., Masucci, M. G. and Dantuma, N. P. (2002) Aggregate formation inhibits proteasomal degradation of polyglutamine proteins. Hum. Mol. Genet. 11, 2689–700.
39 Rubinsztein, D. C. (2006) The roles of intracellular protein-degradation pathways in neurodegeneration. Nature 443, 780–6.
40 Kovacs, A. L., Reith, A. and Seglen, P. O. (1982) Accumulation of autophagosomes after inhibition of hepatocytic protein degradation by vinblastine, leupeptin or a lysosomotropic amine. Exp. Cell Res. 137, 191–201.
41 Kochl, R., Hu, X. W., Chan, E. Y. and Tooze, S. A. (2006) Microtubules facilitate autophagosome formation and fusion of autophagosomes with endosomes. Traffic 7, 129–45.
42 Bohley, P. and Seglen, P. O. (1992) Proteases and proteolysis in the lysosome. Experientia 48, 151–7.
43 Seglen, P. O. and Gordon, P. B. (1982) 3-Methyladenine: Specific inhibitor of autophagic/lysosomal protein degradation in isolated rat hepatocytes. Proc. Natl. Acad. Sci. USA 79, 1889–92.
44 Rujano, M. A., Bosveld, F., Salomons, F. A., Dijk, F., van Waarde, M. A., van der Want, J. J., de Vos, R. A., Brunt, E. R., Sibon, O. C. and Kampinga, H. H. (2006) Polarised asymmetric inheritance of accumulated protein damage in higher eukaryotes. PLoS Biol 4, e417.
45 Kamimoto, T., Shoji, S., Hidvegi, T., Mizushima, N., Umebayashi, K., Perlmutter, D. H. and Yoshimori, T. (2006) Intracellular inclusions containing mutant alpha 1-antitrypsin Z are propagated in the absence of autophagic activity. J. Biol. Chem. 281, 4467–76.
46 Fujita, E., Kouroku, Y., Isoai, A., Kumagai, H., Misutani, A., Matsuda, C., Hayashi, Y. K. and Momoi, T. (2007) Two endoplasmic reticulum-associated degradation (ERAD) systems for the novel variant of the mutant dysferlin: Ubiquitin/proteasome ERAD(I) and autophagy/lysosome ERAD(II). Hum. Mol. Genet. 16, 618–29.
47 Feldman, D., Swarm, R. L. and Becker, J. (1980) Elimination of excess smooth endoplasmic reticulum after phenobarbital administration. J. Histochem. Cytochem. 28, 997–1006.
48 Orci, L., Brown, M. S., Goldstein, J. L., Garcia-Segura, L. M. and Anderson, R. G. (1984) Increase in membrane cholesterol: A possible trigger for degradation of HMG CoA reductase and crystalloid endoplasmic reticulum in UT-1 cells. Cell 36, 835–45.
49 Lucocq, J. M., Brada, D. and Roth, J. (1986) Immunolocalization of the oligosaccharide trimming enzyme glucosidase II. J. Cell Biol. 102, 2137–46.
50 Strous, G. J., Van Kerkhof, P., Brok, R., Roth, J. and Brada, D. (1987) Glucosidase II, a protein of the endoplasmic reticulum with high mannose oligosaccharide chains and a rapid turnover. J. Biol. Chem. 262, 3620–5.
51 Wu, Y., Termine, D., Swulius, M., Moremen, K. and Sifers, R. (2007) Human endoplasmic reticulum mannosidase I is subject of regulated proteolysis. J. Biol. Chem. 282, 4841–9.
52 Zwickl, P., Baumeister, W. and Steven, A. (2000) Dis-assembly lines: The proteasome and related ATPase-assisted proteases. Curr. Opin. Struct. Biol. 10, 242–50.
53 Roy, S., Yu, S., Banerjee, D., Overton, O., Mukhopadhyay, G., Oddoux, C., Grieninger, G. and Redman, C. (1992) Assembly and secretion of fibrinogen. Degradation of individual chains. J. Biol. Chem. 267, 23151–8.
54 Xia, H. and Redman, C. (1999) The degradation of nascent fibrinogen chains is mediated by the ubiquitin proteasome pathway. Biochem. Biophys. Res. Commun. 261, 590–7.
55 Xia, H. and Redman, C. M. (2001) Differential degradation of the three fibrinogen chains by proteasomes: Involvement of Sec61p and cytosolic Hsp70. Arch. Biochem. Biophys. 390, 137–45.
56 Ploegh, H. L. (2007) A lipid-based model for the creation of an escape hatch from the endoplasmic reticulum. Nature 448, 435–8.
57 Tirosh, B., Furman, M. H., Tortorella, D. and Ploegh, H. L. (2003) Protein unfolding is not a prerequisite for endoplasmic reticulum-to-cytosol dislocation. J. Biol. Chem. 278, 6664–72.